



Title	Application of Imaging Technology to Humans
Author(s)	Matsui, Takahiro; Ishii, Masaru
Citation	Make Life Visible. 2019, 3(5909), p. 213-218
Version Type	VoR
URL	<a href="https://hdl.handle.net/11094/93180">https://hdl.handle.net/11094/93180</a>
rights	© 2020 The Author(s) This article is licensed under a Creative Commons Attribution 4.0 International License.
Note	

*The University of Osaka Institutional Knowledge Archive : OUKA*

<https://ir.library.osaka-u.ac.jp/>

The University of Osaka

# Chapter 21

## Application of Imaging Technology to Humans



Takahiro Matsui and Masaru Ishii

### 21.1 Introduction

Through the history of clinical medicine, detailed observation of patient symptoms has been most important for both diagnosis and treatment, and several attempts to observe the human body more precisely have been conducted for a long time. Of the numerous brilliant inventions, histopathology established by Rudolf Ludwig Karl Virchow continues to occupy the central position of definite diagnosis. However, there still exist some problems with typical histopathological diagnostic procedures. First, histological analysis with biopsy procedure inevitably needs some tissue damage. Second, it takes much time to make a diagnosis after biopsy because of the various steps necessary to make pathological specimens, such as fixation, dehydration, embedding, and staining. Therefore, it is desirable to develop a new histological diagnostic system for use in real time, with a less invasive way. On the other hands, the development of imaging technology has greatly influenced life science research in recent years. Especially, intravital imaging technique has a strong impact because it enables to observe life phenomena visually while keeping animals alive. Multiphoton excitation microscopy (MPM) is one of the major tools used to observe deep regions of the living body using fluorescence and multiphoton absorption process. In the field of life science research, MPM is now widely used for intravital imaging of deep tissues such as brain (Meyer-Luehmann et al. 2008) and bone marrow (Ishii et al. 2009). Now life science and clinical medicine are inseparably connected, and the development of new imaging techniques such as MPM recalls the application to humans in the field of clinical medicine. Especially, malignant neoplasms are extremely important diseases that continue to be a major cause of death all over the world, and have a large number of patients. So detailed diagnosis of

---

T. Matsui · M. Ishii (✉)

Department of Immunology and Cell Biology, Osaka University Graduate School of Medicine, Suita, Osaka, Japan  
e-mail: [mishii@icb.med.osaka-u.ac.jp](mailto:mishii@icb.med.osaka-u.ac.jp)

cancer at the cellular level through the application of imaging technology is thought to be of great interest all over the world and have much potential demand. However, there are many obstacles before application of MPM to the clinic. One of the most serious hurdles is that it is difficult to label fluorescently cells in human body, because fluorescent dyes are often toxic. It is obviously impossible as well to perform genetic fluorescent labeling unlike laboratory animals such as mice. In recent years, several articles have been reported the methods of imaging living tissues that do not require any labeling. For example, Raman spectroscopy obtains images by detecting Raman scattered light generated when a sample is irradiated with laser light. Depending on the vibrational properties and component distribution such as proteins, lipids, DNA and so on, image contrast generates without any labeling (Freudiger et al. 2008). Photoacoustic microscopy is also known as an efficient tool for non-labeling imaging. It images tissue by photoacoustic effect, a phenomenon in which molecules absorbing light energy emit heat and acoustic waves are generated by volume expansion due to the heat (Yao et al. 2015). There are some reports indicating the usefulness of imaging for human using these techniques described above (Ji et al. 2013; Hsu et al. 2016), and these facts recall the possible utility of non-labeling MPM (NL-MPM) imaging for human. Moreover, fluorescent imaging including MPM is considered superior to these techniques in spatiotemporal resolution. Here, we introduce our attempt of colorectal carcinoma diagnosis by non-labeling imaging for human colorectal tissues using MPM (Matsui et al. 2017).

## 21.2 MPM Technique Enables to Visualize the Histological Features of Fresh, Unstained Human Colorectal Mucosa and Can Be Used for Histopathological Diagnoses

First, imaging analysis of fresh, unstained normal human colorectal mucosal tissues was performed with an MPM imaging system under 780 nm excitation. Without any labeling, it was possible to visualize the histological features of the colorectal tissues in detail, such as ductal structures of epithelial cells and hematopoietic cells in the lamina propria (Fig. 21.1a). In the NL-MPM images, we were able to recognize three different components by the different color patterns: epithelial cells, hematopoietic cells, and basement membrane. Spectral analyses revealed that auto-fluorescent substances and second harmonic generation (SHG), which is a nonlinear optical phenomenon, made color variation among those three components and made MPM images. The images of our NL-MPM imaging for fresh tissue and conventional hematoxylin and eosin (HE) staining procedures for fixed sections were morphologically very similar (Fig. 21.1b). Such similarity was also observed in NL-MPM imaging of colorectal carcinoma tissue, which showed irregular and atypical ductal structure and nuclear enlargement in epithelial cells like HE staining

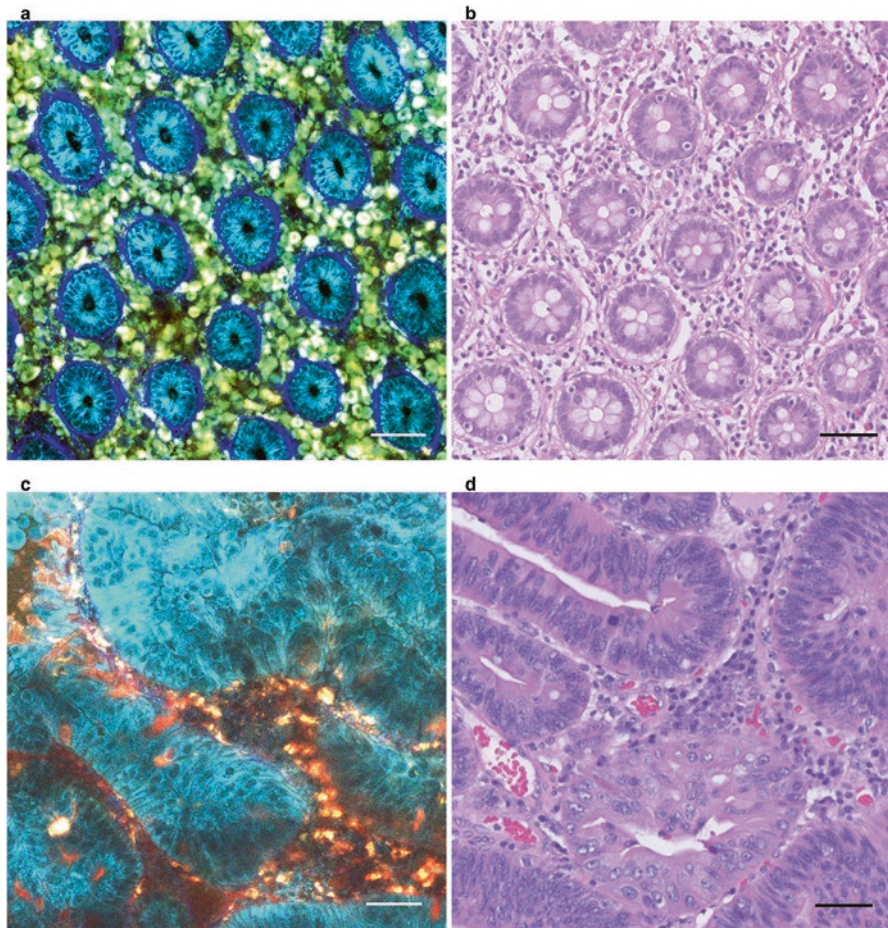


**Fig. 21.1** Non-labeling MPM imaging of human normal colorectal mucosa and colorectal carcinoma. **(a)** MPM imaging of human normal colorectal mucosa. **(b)** HE staining of normal colorectal mucosa, using the same sample as in **(a)**. **(c)** MPM images of colorectal cancer tissue. **(d)** HE-stained images of colorectal cancer tissue, using the same samples as in **(c)**. Bar: 50  $\mu$ m. (These figures were quoted from Matsui et al. 2017)

images (Fig. 21.1c, d). These facts made us to think that it might be possible to perform histopathological diagnosis by NL-MPM imaging, instead of HE staining. In fact, it was possible for experienced pathologists to make correct diagnoses based only on the NL-MPM images in the blind manner. These facts indicated that NL-MPM images of fresh unstained colorectal tissues were as useful as conventional HE staining of resected/fixed specimens for differential diagnosis of cancerous versus non-cancerous regions.

### 21.3 Classification by Numerical Parameters Enables to Distinguish NL-MPM Images to Normal and Cancerous Tissues Quantitatively

One of the most important advantages of fluorescent images is the ability to perform quantitative analyses. It is relatively easy to measure and analyze fluorescent signals compared to bright-field images of HE staining (Kikuta et al. 2013; Egawa et al. 2013). This means that we are able to perform histopathological diagnosis immediately and quantitatively by using MPM images. In order to handle image data quantitatively, it is necessary to extract numerical parameters from the images. In this colorectal NL-MPM imaging, two independent numerical parameters were established: nuclear diameters of epithelial cells and intensity of SHG signal from basement membrane. Nuclear diameters in cancer tissues were statistically larger than those in non-cancerous tissues, while SHG signals from basement membrane were diminished in cancer region compared to normal mucosa. Using both NL-MPM imaging and spectral analysis, these features could easily be quantified and defined as index N (represent nuclear diameters) and index S (represent the intensity of SHG signals), respectively. In examination with multiple samples, most of NL-MPM images of the non-cancerous areas showed low index N and high index S values. In contrast, most areas from cancer lesions showed high index N and low index S values. After threshold values are set from these results, the utility of these two indices as diagnostic tools for distinguishing normal and malignant lesions in colorectal mucosa was evaluated, which showed 96% sensitivity and 84% specificity, respectively (Fig. 21.2). The kappa coefficient between the HE-based conventional diagnosis and the two indices described above was 0.82. From these results, it was shown that we could distinguish cancerous and non-cancerous tissues in fresh, human unstained colorectal mucosa quantitatively, using MPM images and the two indices.

### 21.4 Conclusion

We have described the diagnostic approach of cancer tissue using NL-MPM imaging as an example of imaging technology application to humans. Although we described the analysis of colon tissue, similar analysis is possible in other organs, depending on the distribution of auto-fluorescent substances as well as the degree of nonlinear optical phenomena (Ulrich et al. 2013; Miyamoto and Kudoh 2013). The usefulness of observing and diagnosing human tissues with imaging system lies in its rapidity and quantitativeness. Deep observation capability is also another useful advantage for MPM imaging, although the observation range is limited now (up to typical depth of 120  $\mu\text{m}$  in colorectal mucosa). In life science research, imaging technologies have made it possible to perform quantitative assessment of life phenomena in real time, and have contributed greatly to elucidation of life phenomena.

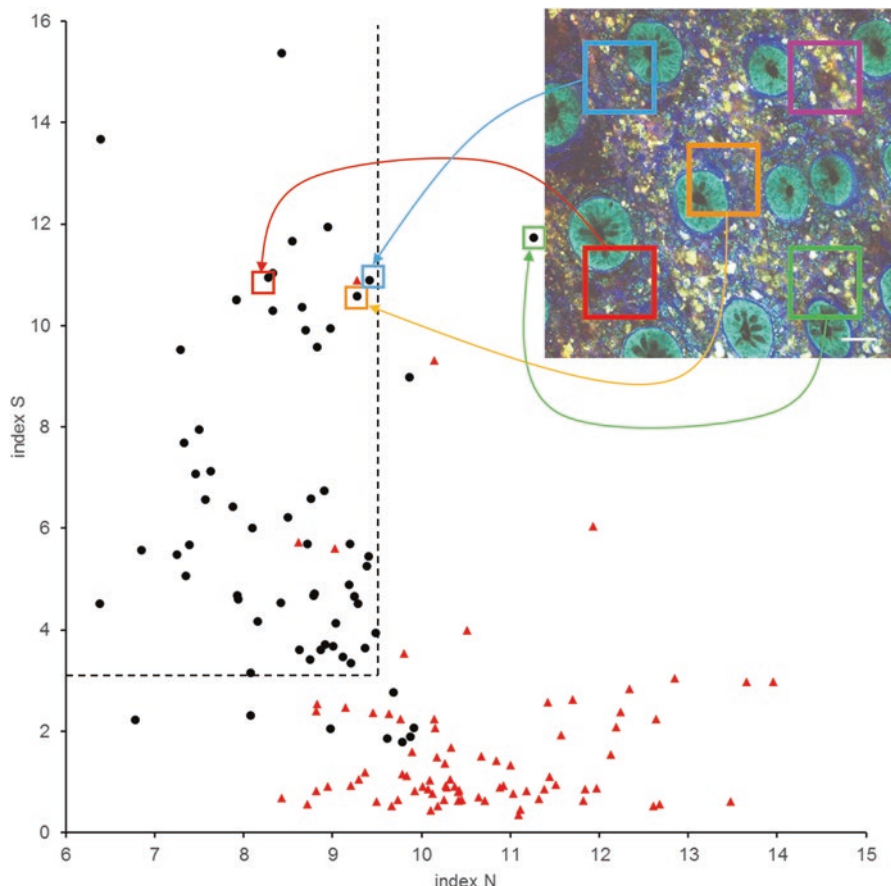


**Fig. 21.2** Classification analysis of MPM images from normal and cancer tissues using the two indices N and S. Five areas (square ROI with a side length of 100  $\mu\text{m}$ ) were determined in advance in the x-y coordinate plane for the original image files, the two indices N and S were calculated with each ROI, and scatter plot was drawn. Final diagnoses of normal (black dot,  $n = 64$ ) or cancer tissue (red triangle,  $n = 80$ ) were made using HE-stained sections from the same specimens imaged by MPM. Areas that showed an index  $N \leq 9.5$  and index  $S > 3.1$  (upper left area of the dashed line) were deemed normal in the classification analysis. Areas that contained no epithelial cell nuclei in the ROI (e.g., the pink ROI) were omitted from the analysis. Bar: 50  $\mu\text{m}$ . (This figure was quoted from Matsui et al. 2017)

The usefulness of imaging procedures is also considered high in experiments targeting humans and clinical medicine. We hope that further development of imaging technology will introduce the breakthrough into clinical medicine as well and contribute to the happiness of humans.

## References

Egawa G, Nakamizo S, Natsuaki Y, Doi H, Miyachi Y, Kabashima K (2013) Intravital analysis of vascular permeability in mice using two-photon microscopy. *Sci Rep* 3:1932. <https://doi.org/10.1038/srep01932>

Freudiger CW, Min W, Saar BG, Lu S, Holtom GR, He C et al (2008) Label-free biomedical imaging with high sensitivity by stimulated Raman scattering microscopy. *Science* 322(5909):1857–1861. <https://doi.org/10.1126/science.1165758>

Hsu HC, Wang L, Wang LV (2016) In vivo photoacoustic microscopy of human cuticle microvasculature with single-cell resolution. *J Biomed Opt* 21(5):56004. <https://doi.org/10.1117/1.JBO.21.5.056004>

Ishii M, Egen JG, Klauschen F, Meier-Schellersheim M, Saeki Y, Vacher J et al (2009) Sphingosine-1-phosphate mobilizes osteoclast precursors and regulates bone homeostasis. *Nature* 458(7237):524–528. <https://doi.org/10.1038/nature07713>

Ji M, Orringer DA, Freudiger CW, Ramkisson S, Liu X, Lau D et al (2013) Rapid, label-free detection of brain tumors with stimulated Raman scattering microscopy. *Sci Transl Med* 5(201):201ra119. <https://doi.org/10.1126/scitranslmed.3005954>

Kikuta J, Wada Y, Kowada T, Wang Z, Sun-Wada GH, Nishiyama I et al (2013) Dynamic visualization of RANKL and Th17-mediated osteoclast function. *J Clin Invest* 123(2):866–873. <https://doi.org/10.1172/JCI65054>

Matsui T, Mizuno H, Sudo T, Kikuta J, Haraguchi N, Ikeda JI et al (2017) Non-labeling multi-photon excitation microscopy as a novel diagnostic tool for discriminating normal tissue and colorectal cancer lesions. *Sci Rep* 7(1):6959. <https://doi.org/10.1038/s41598-017-07244-2>

Meyer-Luehmann M, Spires-Jones TL, Prada C, Garcia-Alloza M, de Calignon A, Rozkalne A et al (2008) Rapid appearance and local toxicity of amyloid-beta plaques in a mouse model of Alzheimer's disease. *Nature* 451(7179):720–724. <https://doi.org/10.1038/nature06616>

Miyamoto K, Kudoh H (2013) Quantification and visualization of cellular NAD(P)H in young and aged female facial skin with in vivo two-photon tomography. *Br J Dermatol* 169(Suppl 2):25–31. <https://doi.org/10.1111/bjd.12370>

Ulrich M, Klemp M, Darvin ME, Konig K, Lademann J, Meinke MC (2013) In vivo detection of basal cell carcinoma: comparison of a reflectance confocal microscope and a multiphoton tomograph. *J Biomed Opt* 18(6):61229. <https://doi.org/10.1117/1.JBO.18.6.061229>

Yao J, Wang L, Yang JM, Maslov KI, Wong TT, Li L et al (2015) High-speed label-free functional photoacoustic microscopy of mouse brain in action. *Nat Methods* 12(5):407–410. <https://doi.org/10.1038/nmeth.3336>

**Open Access** This chapter is licensed under the terms of the Creative Commons Attribution 4.0 International License (<http://creativecommons.org/licenses/by/4.0/>), which permits use, sharing, adaptation, distribution and reproduction in any medium or format, as long as you give appropriate credit to the original author(s) and the source, provide a link to the Creative Commons licence and indicate if changes were made.

The images or other third party material in this chapter are included in the chapter's Creative Commons licence, unless indicated otherwise in a credit line to the material. If material is not included in the chapter's Creative Commons licence and your intended use is not permitted by statutory regulation or exceeds the permitted use, you will need to obtain permission directly from the copyright holder.

